Food and Chemical Toxicology 129 (2019) 337–343

Contents lists available at ScienceDirect

Food and Chemical Toxicology

journal homepage: www.elsevier.com/locate/foodchemtox

# Anthraquinone-type inhibitor of α-glucosidase enhances glucose uptake by activating an insulin-like signaling pathway in C2C12 myotubes

Md Badrul Alam[a,1], Vivek K. Bajpai[b,1], Jeong-Sic Ra[a], Ji-Young Lim[a], Hongyan An[a], Shruti Shukla[b], Khong Trong Quan[c], Imran Khan[d], Yun Suk Huh[d,*], Young-Kyu Han[b,**], MinKyun Na[c,***], Sang-Han Lee[a,****]

[a] Department of Food Science and Biotechnology, Graduate School, Kyungpook National University, Daegu, 41566, South Korea
[b] Department of Energy and Materials Engineering, Dongguk University-Seoul, Seoul, 04620, Republic of Korea
[c] College of Pharmacy, Chungnam National University, Daejeon, 34134, Republic of Korea
[d] Department of Biological Engineering, Biohybrid Systems Research Center (BSRC), Inha University, 100 Inha-ro, Nam-gu, Incheon, 22212, Republic of Korea

ARTICLE INFO

*Keywords:*
Rubia philippinensis
Anthraquinone
Antidiabetic effect
Insulin-like signaling pathway
GLUT4 translocation

ABSTRACT

This study assesses the ability of anthraquinone derivative, 2-methyl-1,3,6-trihydroxy-9,10-anthraquinone (MTAQ) to decrease postprandial hyperglycemia or enhance glucose uptake and to elucidate the underlying molecular mechanism. We investigated α-glucosidase inhibition, glucose uptake, and translocation of glucose transporter 4 (GLUT4) in C2C12 myotubes. The data indicate that MTAQ strongly inhibited α-glucosidase activity in a concentration-dependent manner, with an $IC_{50}$ value of 6.49 ± 1.31 μM, and functioned as a reversible competitive inhibitor, with a dissociation constant of 41.88 μM. Moreover, MTAQ significantly augmented basal and insulin-stimulated glucose uptake as well as translocation of GLUT4 to the plasma membrane. It also stimulated the phosphorylation of insulin receptor β isoform, insulin receptor substrate-1,3-phosphoinositide-dependent protein kinase 1, and protein kinase B (AKT). A pretreatment with an AKT inhibitor, LY294002, attenuated the ability of MTAQ to activate an insulin-like signaling pathway and to enhance basal and insulin-stimulated glucose uptake and stimulate GLUT4 translocation to the plasma membrane. These findings reveal the fact that MTAQ may have potential for the development of new antidiabetic drugs to manage blood glucose levels.

## 1. Introduction

Diabetes mellitus (DM) is characterized by fasting and postprandial hyperglycemia and known as a complex metabolic disorder. It occurs when the pancreas does not produce the optimal level of insulin or the body develops insulin resistance. (Tundis et al., 2010). DM is a major health risk worldwide. Globally, the DM population is going to increase to 439 million by 2030, with 90% of those affected having type-2 diabetes mellitus (T2-DM) (Whiting et al., 2011). A characteristic feature of T2-DM is insulin resistance, whereby the major insulin-sensitive tissues, such as skeletal muscle, liver, and adipose tissue, become resistant to insulin. This insensitivity to insulin ultimately results in decreased glucose utilization in the peripheral tissue and increased blood glucose levels (S. Huang and Czech, 2007; Zhou et al., 2008).

Uptake of glucose by skeletal muscles is mediated mainly *via* two major pathways. In the first pathway known as insulin-dependent pathway, insulin activates to the insulin receptor (IR) to trigger other signaling pathways [e.g., glucose transporter 4 (GLUT4) translocation; atypical protein kinase C; protein kinase B (AKT); phosphoinositide 3-kinase (PI3K); and IR substrate (IRS)] that enhance glucose uptake by skeletal muscles (Hesselink et al., 2016). Consequently, adequate production of insulin in β-cells and sensitivity of insulin to relevant tissues are crucial for homeostasis of glucose. The second major pathway is an insulin-independent signaling pathway, which is mediated by a heterotrimeric functional enzyme complex called 5′-adenosine monophosphate-activated protein kinase (AMPK). This pathway is critical for

* Corresponding authors.
** Corresponding author.
*** Corresponding authors.
**** Corresponding author.
*E-mail addresses:* yunsuk.huh@inha.ac.kr (Y.S. Huh), ykenergy@dongguk.edu (Y.-K. Han), mkna@cnu.ac.kr (M. Na), sang@knu.ac.kr (S.-H. Lee).
[1] Equally contributed.

https://doi.org/10.1016/j.fct.2019.05.005
Received 28 December 2018; Received in revised form 3 April 2019; Accepted 4 May 2019
Available online 06 May 2019

metabolic control and the regulation of cellular energy homeostasis. However, postprandial glucose uptake by skeletal muscles is believed to be mediated by GLUT4, which is translocated to the plasma membrane in response to insulin. Decreased intracellular GLUT4 trafficking to the plasma membrane is one of the major causes of T2-DM (Huang and Czech, 2007).

Because of the increasing number of diabetics worldwide, new and effective therapeutic options are needed. The best treatment for T2-DM involves controlling hyperglycemia with appropriate remedies and a healthy life-style. Insulin therapy is currently the best treatment option, and some synthetic small molecules and natural products are reportedly able to mimic the actions of insulin and promote glucose uptake in cell cultures and animal models of diabetes (Echouffo-Tcheugui and Garg, 2017). However, another therapeutic approach for treating diabetes involves decreasing postprandial hyperglycemia. The α-glucosidase enzyme is located in the brush border of the small intestine and is required for the final step in the breakdown of carbohydrates such as starch, dextrin, and maltose to the absorbable monosaccharides. As inhibitors of this enzyme, the α-glucosidase inhibitors delay but do not prevent the absorption of ingested carbohydrates and reduce the postprandial insulin and glucose peaks (Collins, 2002; Ross et al., 2004). Delaying glucose absorption helps to match the pancreatic insulin response and reduces postprandial hyperglycemia. Moreover, the α-glucosidase inhibitors generally lower HbA1c levels by approximately 0.5%–1%. However, the α-glucosidase inhibitors are appealing because they lower postprandial glucose levels by a mechanism that does not require systemic absorption, and they do not cause hypoglycemia or weight gain (Collins, 2002). They are approved for use as monotherapy and in combination with other anti-diabetic agent. Therefore, a combination of a secretagogue or an insulin sensitizer and an α-glucosidase inhibitor may represent a viable alternative to current treatments for diabetes. An α-glucosidase inhibitor is crucial for preventing postprandial glucose spikes, thereby augmenting the effects of the secretagogue or insulin sensitizer as part of a good glycemic control regimen (Maritim et al., 2003).

Natural plant remedies are increasingly used in modern clinical medicine as alternative treatments for T2-DM, with acceptable efficacy and fewer side effects than other available therapeutic options. Another reason for the growing interest in such remedies is that they are generally safe for patients. Examples of medicinal plants include *Rubia philippinensis*, which is a low-climbing and perennial herb that naturally grows only in southern Vietnam and Luzon (Philippines). Although chemical analyses of *R. philippinensis* have been limited (Quan et al., 2016), other *Rubia* species have been characterized in more detail (Xu et al., 2013; Xu et al., 2014). To date, anthraquinones, lignans, triterpenoids, and cyclopeptides have been isolated from *Rubia* species. A number of anthraquinones have been purified and identified as the major constituents of *Rubia akane* (Itokawa et al., 1983). Furthermore, 2-methyl-1,3,6-trihydroxy-9,10-anthraquinone (MTAQ) is the main active component responsible for the anti-hyperlipidemic activity of *Rubia yunnanensis* (Gao et al., 2014).

Researchers have recently attempted to identify natural sources of effective α-glucosidase inhibitors (Ali et al., 2015; Li et al., 2018). These inhibitors may be useful for developing new drugs to treat T2-DM. In this background, the current study was conducted to extract new α-glucosidase inhibitors from a medicinal plant *R. philippinensis* and clarify the effects of MTAQ on glucose uptake in C2C12 myotubes as well as the underlying molecular mechanism. We observed that MTAQ stimulates glucose transport in C2C12 myotubes by inducing the translocation of GLUT4 *via* the activation of insulin-like signaling pathways. These observations may help to elucidate the hypoglycemic and the antidiabetic potential of MTAQ.

## 2. Materials and methods

### 2.1. Drugs and chemicals

α-Glucosidase, p-nitrophenyl-α-D-glucopyranoside (pNPG), 3-(4,5-dimethylthiazol-2-yl)-2,5-diphenyltetrazolium bromide (MTT), LY294002 (AKT inhibitor), and dimethyl sulfoxide (DMSO) were acquired from Sigma-Aldrich (USA). Penicillin-streptomycin mixture, fetal bovine serum (FBS), Dulbecco's modified Eagle's medium (DMEM), and 0.25% trypsin-ethylenediaminetetraacetic acid (EDTA) were procured from GE Healthcare Life Sciences HyClone (Melbourne, Australia). Additionally, 2-NBDG was purchased from Thermo Fisher Scientific Inc. (Carlsbad, CA, USA). Anti-phospho-IRβ (Tyr 1150/1151), and anti-IRβ were purchased from Santa Cruz Biotechnology (CA, USA), whereas anti-phospho-AKT, anti-AKT, anti-phospho-IRS1 (S1101), anti-IRS1, anti-phospho-PDK1, anti-PDK1, anti-GLUT4, and anti-β-actin antibodies were acquired from Bioworld Technology Inc. (MN, USA).

### 2.2. Plant materials

*Rubia philippinensis* root samples were obtained from the Lamdong National Park (Vietnam), and samples were stored at the laboratory of the National Institute of Medicinal Materials (NIMM), Hanoi, Vietnam and authenticated by the botanical scientist Dr. Phuong Thien Thuong. A voucher (VDL20140801) of *R. philippinensis* root specimen sample was preserved at the NIMM laboratory as well as at the Laboratory of Pharmacognosy, Chungnam National University, Daejeon, Korea under the voucher specimen number CNU1409.

### 2.3. Extraction and isolation of anthraquinone derivatives

Five anthraquinones, 2-methyl-1,3,6-trihydroxy-9,10-anthraquinone-3-*O*-(6′-*O*-acetyl)-α-rhamnosyl(1 → 2)-β-glucoside (**1**), 2-methyl-1,3,6-trihydroxy-9,10-anthraquinone (**2**), alizarin (**3**), xanthopurpurin (**4**), and lucidin-ω-methyl ether (**5**), were available from our previous chemical study (Bajpai et al., 2018).

### 2.4. α-Glucosidase inhibitory assay

The α-glucosidase inhibitory activity of isolated compounds (**1–5**) was measured as described by Zhao et al. (2017). Briefly, 2 μL predetermined concentration of various isolates, including MTAQ, was mixed with 0.2 U/mL α-glucosidase in 0.1 M sodium phosphate buffer (pH 7.0). The substrate, pNPG (2 mM), was subsequently added to the solution to initiate the enzymatic reactions at 37 °C for 30 min. The α-glucosidase inhibitory activity was measured spectrophotometrically at 405 nm using a 96-well plate and the Victor3 microplate reader (PerkinElmer, Waltham, MA, USA). Acarbose, which is a competitive α-glucosidase inhibitor, served as the positive control. The below mentioned equation was employed to calculate the inhibitory percentage:

$$\alpha\text{-Glucosidase activity (\% inhibition)} = [(Abs_{control} - Abs_{sample})/Abs_{control}] \times 100$$

The kinetics underlying the inhibition of α-glucosidase by MTAQ were determined with a series of sample solutions with varying substrate concentrations. The solutions were prepared without MTAQ or with MTAQ at different concentrations. The mode of inhibition of MTAQ was assessed using a Lineweaver–Burk plot, and the Km (dissociation constant) and Vmax (maximum reaction velocity) of the enzyme were calculated (Gong et al., 2017).

### 2.5. Cell culture and cell viability assay

We cultured C2C12 cells (American Type Culture Collection, Manassas, VA, USA) in DMEM supplemented with FBS (10%) and

penicillin (100 U/mL)-streptomycin (100 μg/mL) at 37 °C under humid conditions with 5% $CO_2$. The tetrazolium dye colorimetric test involving MTT was used to assess C2C12 cell viability. At first, the cells were cultured in a 96-well plate ($1 \times 10^5$ cells/well) for 24 h. After reaching 90% confluence, cells were treated with various concentrations of MTAQ, where the final concentration of DMSO was ≤0.1%. Controls were treated with DMEM medium with a final concentration of 0.1% of DMSO but without MTAQ. Following the incubation of 24 h, the MTT reagent was added to each well, followed by incubating the plate at 37 °C for 1 h. Then the medium was subjected to remove, and the wells were washed two-times using PBS (pH 7.4). Then the insoluble intracellular formazan was dissolved in DMSO (100%) followed by measurement of absorbance of each well at 570 nm using the Victor3 microplate reader. Cell viability was then calculated as a percentage.

### 2.6. Cell differentiation and glucose uptake assay

We cultured C2C12 cells in 96-well plates ($1 \times 10^5$ cells/well) containing DMEM supplemented with 10% FBS and 1% penicillin-streptomycin. The plates were incubated at 37 °C, with 5% $CO_2$. After reaching full confluence, cells were differentiated for 5 days in DMEM supplemented with 2% horse serum. The cells were then starved in low-glucose serum-free DMEM for 24 h, after which the 2-NBDG assay was conducted to evaluate glucose uptake (Zhao et al., 2017). Briefly, cells were treated with various concentrations of MTAQ and insulin (100 nM) for specific time intervals before being treated with 20 μM 2-NBDG for 1 h. The cells were subsequently washed three times with cold PBS, and 2-NBDG uptake was measured with the Victor3 microplate reader, with excitation and emission wavelengths of 490 and 535 nm, respectively.

### 2.7. Reverse transcription-polymerase chain reaction (RT-PCR)

C2C12 cells ($1 \times 10^5$ cells/well) were cultured in 6 well plates and the total RNA was extracted from C2C12 cells using TRIzol (Ambion, Austin, TX, USA), according to the manufacturer's instructions (Rozen and Skaletsky, 2000). The extracted RNA (2 μg) was used as the template to prepare cDNA with the RT & GO Mastermix (Biomedicals, Seoul, Korea). The RT-PCR was completed using various primers (Table S1) and the TAKARA's PCR Thermal Cycler Dice system - TP600 (Otsu, Japan). A 2% agarose gel (Tris-acetate-EDTA buffer, 100 V) was used to separate the PCR products for 30 min, and visualization of bands was performed with ethidium bromide. An Image Lab™ software was used for the analysis of DNA bands.

### 2.8. Preparation of cell lysates and western blotting

Ice-cold PBS was employed for washing of C2C12 ($1 \times 10^5$ cells/well) treated with MTAQ. Then the cells were lysed in ice-cold RIPA buffer followed by incubation of the obtained lysates at 4 °C for 30 min. Lysates were then subjected to centrifugation (12,000 rpm; 10 min; 4 °C) for the removal of insoluble proportions. A BCA protein assay kit (Pierce, Rockford, IL, USA) was used to determine the protein concentration, after which 20 μg protein was analyzed by 10% sodium dodecyl sulfate polyacrylamide gel electrophoresis. The separated proteins were transferred to nitrocellulose membranes (Whatman, Dassel, Germany), which were then blocked with 5% non-fat milk in TBST buffer and treated with a primary antibody (1:1000) and the corresponding secondary antibody (1:5000). Protein bands were detected using the SuperSignal West Femto Maximum Sensitivity Substrate (Thermo Fisher Scientific, Rockford, IL, USA). The protein bands were analyzed by Image Lab™ software.

### 2.9. Extraction of plasma membrane proteins

Ice-cold PBS washed cells were then harvested followed by extraction of plasma membrane proteins according to the instruction of plasma membrane protein isolation kit (Abcam PLC, CA, USA). Briefly, cells were homogenized in ice-cold homogenized buffer, followed by centrifugation at 700 × *g* for 10 min at 4 °C. Then the supernatant was collected which was further subjected to centrifugation (10,000 × *g* for 30 min at 4 °C) followed by collection of the supernatant (post-plasma fraction) and the pellet (containing plasma membrane protein). After that, the pellet was re-suspended in upper phase solution followed by addition of lower phase solution and re-centrifuged at 1000 × *g* for 5 min. The upper phase solution was then carefully transferred in a new tube. To maximize the yield, the lower phase solution was again extracted with upper phase solution and centrifuged at 1000 × *g* for 5 min. Then both upper and lower phase solutions were mixed well and the solution was centrifuged at 1000 × *g* for 5 min followed by collection of upper phase solution, and diluted with 5-fold water, followed by spin-down using a micro-centrifuge for 10 min. Finally, the supernatant was discarded and the pellet was considered as the plasma membrane protein. The contents of plasma membrane protein were then determined using a BCA protein assay reagent.

### 2.10. Statistical analysis

Data underwent a one-way analysis of variance, and post-hoc Dunnett's test was used to determine statistical significance and are presented as the mean ± standard deviation. All results were statistically analyzed using Window's SPSS program. Significant differences were determined based on the following thresholds: $p < 0.01$ or $< 0.05$.

## 3. Results

### 3.1. Evaluation of α-glucosidase inhibition and analysis of reaction kinetics

The anthraquinone derivatives (compound 1–5), including MTAQ (Fig. 1) (refer to the supplementary figure S1) were characterized and identified based on the $^1H$ and $^{13}C$ NMR data (Bajpai et al., 2018). Anthraquinone derivatives (**1–5**) inhibited α-glucosidase in a concentration-dependent manner, with $IC_{50}$ values of 41.22 ± 1.13, 6.49 ± 1.31, 21.94 ± 0.89, 84.71 ± 1.21, and 88.49 ± 1.74 μM, respectively. Acarbose, which was used as a positive control, had an $IC_{50}$ value of 165.19 ± 0.20 μM (Fig. 2A and figure S2), suggesting that the small structural differences in the molecules had little impact on enzymatic inhibitory activities.

Of the tested compounds, MTAQ inhibited α-glucosidase activity the most. To confirm the nature of the interaction involving MTAQ, the kinetics of the inhibition of α-glucosidase were analyzed. Lineweaver–Burk plots were constructed based on different MTAQ concentrations. Typical reversible competitive plots were produced for MTAQ (Fig. 2B), with a series of lines with different slopes intersecting the Y-axes. Additionally, the dissociation constant (Ki) was 41.88 μM. The calculated Km and Vmax values are provided in Table 1.

### 3.2. MTAQ stimulates basal and insulin-mediated glucose uptake in C2C12 myotubes

To observe the effects of MTAQ on glucose uptake *in vitro*, insulin-

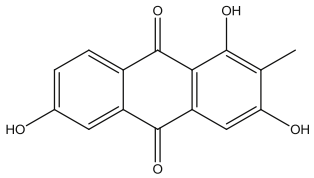


**Fig. 1.** Chemical structures of 2-methyl-1,3,6-trihydroxy-9,10-anthraquinone (MTAQ) obtained from *Rubia philippinensis*.

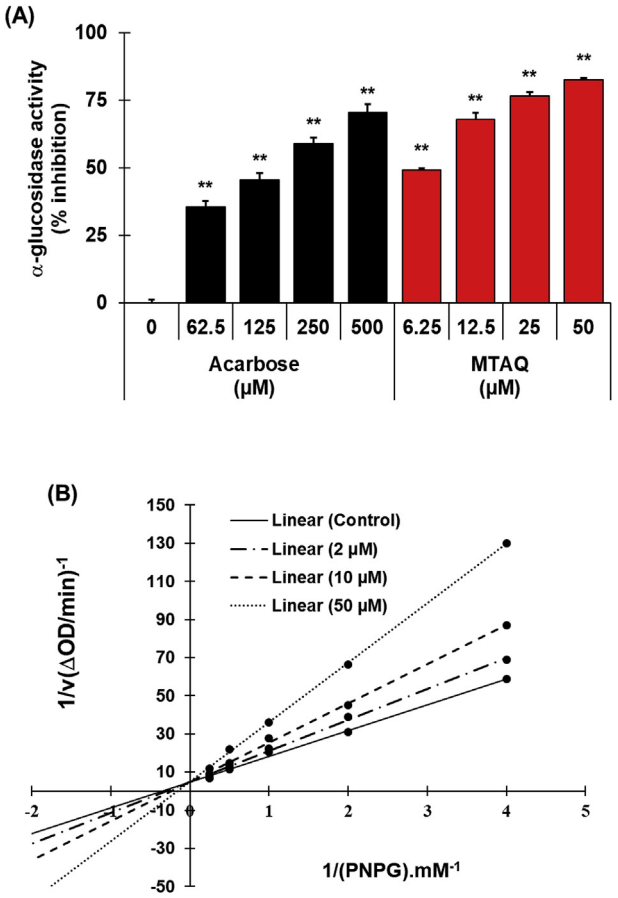


**Fig. 2.** Inhibitory effects of MTAQ on α-glucosidase activity. (**A**) Different concentrations of MTAQ or acarbose were incubated with the same units of α-glucosidase. Following incubation, amounts of p-nitrophenol produced were determined at 405 nm spectrophotometrically. (**B**) Line weaver-Burk plot of α-glucosidase in the presence of MTAQ. Results are expressed as mean values of 1/V, as inverses of increases in absorbance at 405 nm/min ($\Delta A_{405}$ per minute), and as the means of three independent tests at different PNPG concentrations. Results are presented as the means ± SDs of three experiments. *P < 0.05, **P < 0.01, versus non-treated controls.

**Table 1**
Kinetic parameters of α-glucosidase in the presence of MTAQ.

| Compound | Concentration (mM) | Km (mM) | $V_{max}$ ($\Delta A_{405}$ per min) | Mode of inhibition |
|---|---|---|---|---|
| None | – | $2.78 \times 10^{-3}$ | $20.60 \times 10^{-2}$ | |
| MTAQ | $2 \times 10^{-3}$ | $3.34 \times 10^{-3}$ | $20.61 \times 10^{-2}$ | Competitive |
| | $10 \times 10^{-3}$ | $4.22 \times 10^{-3}$ | $20.56 \times 10^{-2}$ | |
| | $50 \times 10^{-3}$ | $6.42 \times 10^{-3}$ | $20.60 \times 10^{-2}$ | |

sensitive mouse skeletal muscle cell line C2C12 myotubes were treated with MTAQ at specific time points. Exposure to 50 μM MTAQ induced basal or insulin-stimulated glucose uptake starting at 1 h, with a peak observed at 2 h, followed by a gradual decrease (Fig. 3A). Thus, in the present study, the 2 h time point was selected for MTAQ treatments in subsequent experiments. Fig. 3B indicates that basal or insulin-stimulated glucose uptake increased in a concentration-dependent manner, with no signs of toxicity (figure S3). The highest MTAQ concentration (50 μM) significantly increased basal and insulin-stimulated glucose uptake by 39 ± 4.9% and 36 ± 5.7%, respectively. Additionally, rosiglitazone (i.e., an antidiabetic agent belonging to the thiazolidinedione class) was used as a positive control, and significantly increased the basal and insulin-stimulated glucose uptake by 27 ± 4.2% and 21 ± 4.4%, respectively.

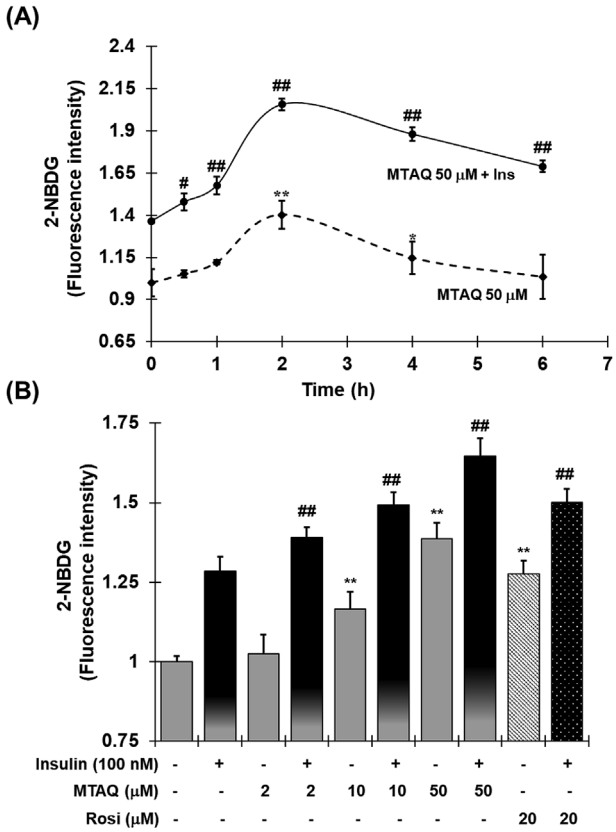


**Fig. 3.** Effects of MTAQ on glucose uptake in C2C12 myotubes. (**A**) Time course of the effect of MTAQ on glucose uptake in C2C12 myotubes. Cells were treated with MTAQ (50 μM) alone or MTAQ (50 μM), followed by insulin (100 nM) for 30 min, and then incubated for the time periods indicated. (**B**) The dose−response relationship of the effects of MTAQ on glucose uptake in C2C12 myotubes. Cells were treated with MTAQ for 2 h. Rosiglitazone (20 μM) were used as positive controls. Results are expressed as means ± SEM of three independent experiments, each performed in triplicate. *p < 0.05 and **p < 0.01, vs basal glucose uptake (no insulin stimulation); #p < 0.05 and ##p < 0.01, vs insulin-stimulated glucose uptake. Rosi: Rosiglitazone.

### 3.3. MTAQ promotes the translocation of GLUT4 in C2C12 cells

The ability of MTAQ to increase glucose transport in C2C12 myotubes was correlated with increased GLUT4 translocation, and the GLUT4 mRNA levels were measured. Additionally, the GLUT4 contents in the plasma membrane and post-plasma membrane fractions in the absence or presence of MTAQ and insulin were examined by the western blot. Interestingly, MTAQ significantly increased the GLUT4 mRNA level in a concentration-dependent manner (Fig. 4A). The western blot results (Fig. 4B) revealed that MTAQ increased the translocation of GLUT4 in both basal and insulin-stimulated situations. Additionally, the MTAQ treatment enhanced the translocation of GLUT4 to the plasma membrane in a concentration-dependent manner (Fig. 4C).

### 3.4. MTAQ mimics an insulin signal in C2C12 cells

To investigate whether MTAQ increases glucose uptake by activating the insulin-signaling pathway, the activation of IR, IRS-1, and 3-phosphoinositide-dependent protein kinase 1 (PDK1) was assessed by RT-PCR and western blot analysis. The MTAQ treatment significantly increased the transcription of the genes encoding IR, IRS-1, and PDK1 in a concentration-dependent manner (Fig. 5A). As expected, the phosphorylation of IRβ, IRS-1, and PDK1 was significantly augmented by MTAQ alone and in insulin-stimulated cells (Fig. 5B). The relative extent of the phosphorylation of IRβ, IRS-1, and PDK1 is presented in

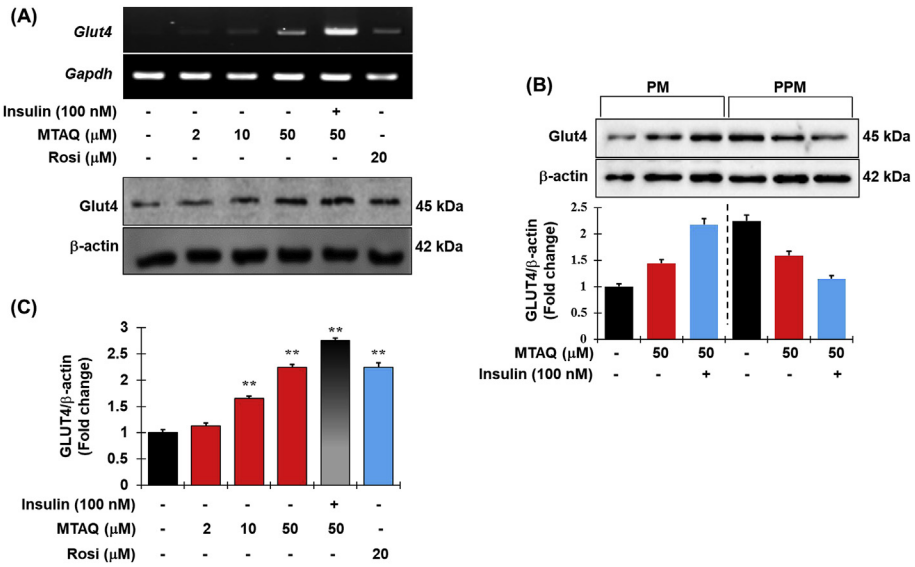


**Fig. 4.** Effect of MTAQ on the translocation of GLUT4 in C2C12 myotubes. (**A**) Cells were treated with indicated concentration of MTAQ alone or MTAQ (50 μM), followed by insulin (100 nM) for 30 min, and then incubated for 2 h mRNA was extracted using TRIzol and mRNA expressions was analyzed by RT PCR. (**B and C**) Subcellular membrane fractions were extracted and subjected to immunoblot analysis with the indicated antibodies. Statistical data were represented in the adjacent figure. Values are means ± SEM of three independent experiments. **p < 0.01 vs no treatment. Rosi: Rosiglitazone.

Fig. 5C. Moreover, to observe whether MTAQ can also enhance the activation of AKT, which is another key signaling molecule for insulin-mediated GLUT4 translocation, we examined the time- and concentration-dependent phosphorylation of AKT in an immunoblot. The MTAQ treatment augmented the phosphorylation of AKT starting at 30 min, with a peak at 2 h (Fig. 6A). Additionally, MTAQ significantly enhanced the phosphorylation of AKT in a concentration-dependent manner (Fig. 6B). However, MTAQ did not significantly affect the phosphorylation of AMPK (figure S4). Thus, our data suggested that MTAQ significantly activates the insulin-signaling pathway, resulting in enhanced GLUT4 translocation and glucose uptake.

Furthermore, to investigate whether the phosphorylation of AKT by MTAQ is associated with the increased GLUT4 translocation to the plasma membrane to enhance glucose uptake, we examined the effects of LY294002, which is a selective inhibitor of AKT. We observed that LY294002 significantly blocked the AKT phosphorylation, even after treatment of MTAQ in the absence or presence of insulin (figure S5). Additionally, the GLUT4 translocation induced by MTAQ in the absence or presence of insulin was significantly attenuated in C2C12 myotubes when AKT was inhibited (Fig. 6C). Moreover, LY294002 significantly suppressed the ability of MTAQ to enhance glucose uptake. The increases in the basal and insulin-stimulated glucose uptake induced by 50 μM MTAQ were significantly decreased by LY294002 to 26.3% and 40.0%, respectively (Fig. 6D). These results implied that the signaling pathway of AKT crucially acts in the increased uptake of glucose mediated by MTAQ.

## 4. Discussion

As a complicated metabolic disorder, diabetes mellitus has become a serious health issue worldwide. Insulin, prandial glucose regulators, insulin sensitizers, and insulin-secretagogues are used alone or in combination to improve glycemic regulation; however, many of these drugs can induce severe side effects in patients with poor tolerance (Echouffo-Tcheugui and Garg, 2017). Thus, alternative hypoglycemic agents that cause fewer side effects are needed. There is increasing

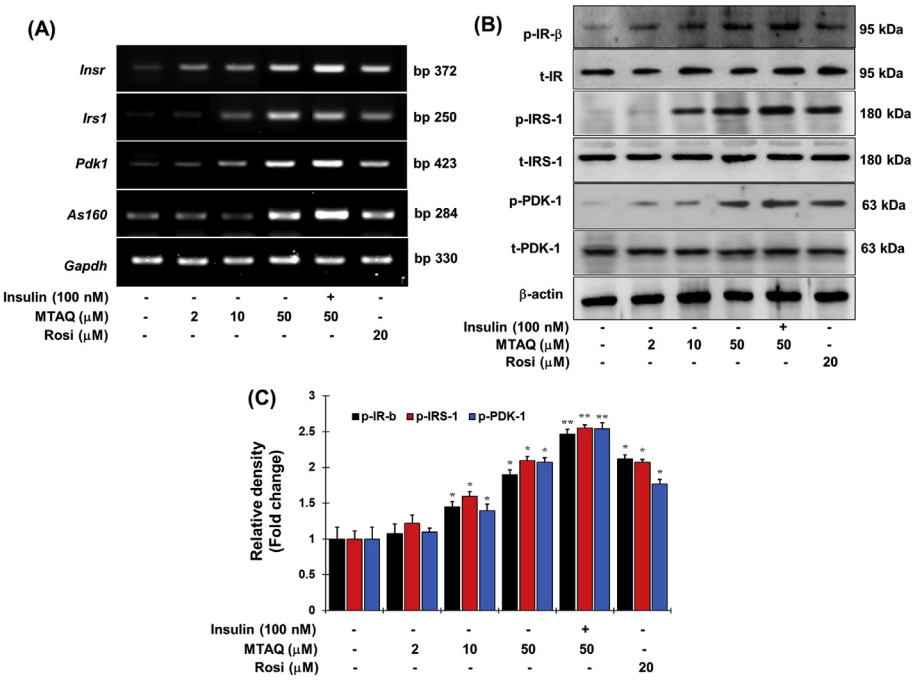


**Fig. 5.** Effect of MTAQ on the insulin-signaling pathway in C2C12 myotubes. (**A**) Cells were treated with indicated concentration of MTAQ alone or MTAQ (50 μM), followed by insulin (100 nM) for 30 min, and then incubated for 2 h mRNA was extracted using TRIzol and mRNA expressions was analyzed by RT-PCR. (**B**) Total cell lysates were extracted and subjected to immunoblot analysis with the indicated antibodies (**C**) The immunoblotting signals of the indicated proteins for MTAQ alone and with insulin from three independent experiments were quantified using densitometer. Data represent means ± SEM, *p < 0.05 and **p < 0.01, vs no treatment. Rosi: Rosiglitazone.

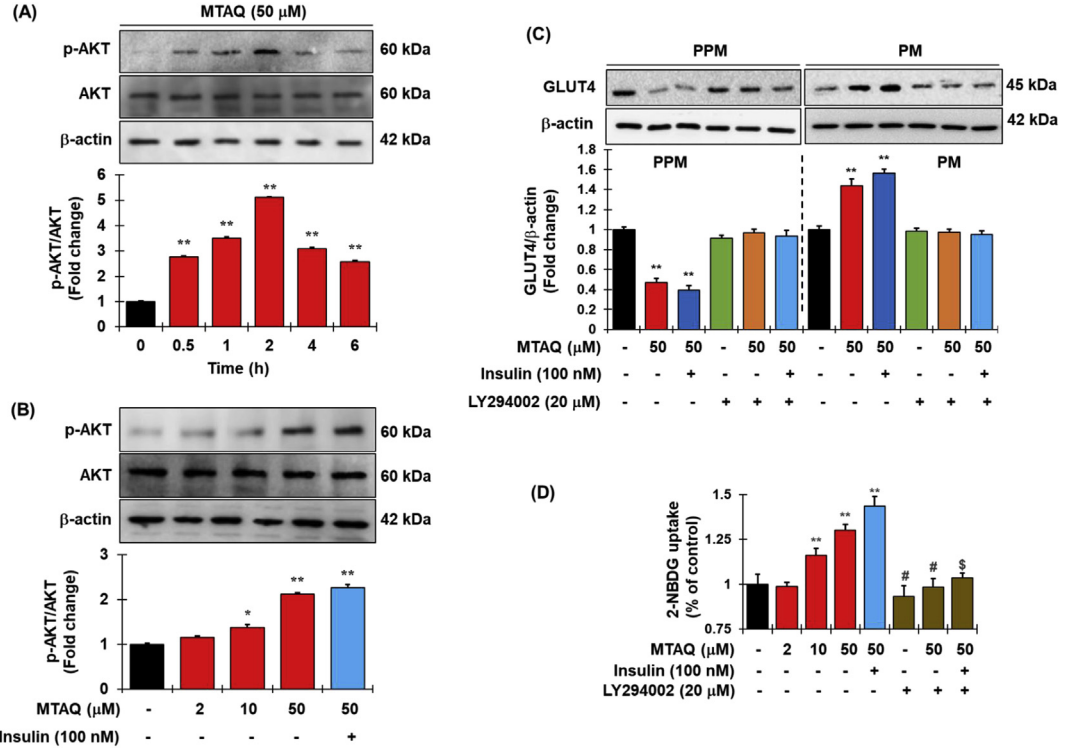


**Fig. 6.** Involvement of the Akt-mediated pathway in MTAQ-induced stimulation of glucose uptake. (A) Time course of the effect of MTAQ on AKT phosphorylation in C2C12 myotubes. Cells were treated with MTAQ (50 μM) and then incubated for the time periods indicated. Statistical data were represented in the adjacent figure. Values are means ± SEM of three independent experiments. **p < 0.01 vs no treatment. (B) C2C12 myotubes were incubated with various concentrations of MTAQ alone for 2 h, or MTAQ (50 μM) for 2 h followed by insulin (100 nM) for 30 min. Cell lysates were resolved by SDS-PAGE, and immunoblotting was performed. Statistical data were represented in the adjacent figure. Values are means ± SEM of three independent experiments. **p < 0.01 vs no treatment. (C) Effects of LY294002 on the translocations of GLUT4 induced by MTAQ in C2C12 myotubes. Subcellular membrane fractions were extracted and subjected to immunoblot analysis. Statistical data were represented in the adjacent figure. Values are means ± SEM of three independent experiments. **p < 0.01 vs no treatment (D) Effect of MTAQ on glucose uptake in LY294002-pretreated C2C12 myotubes. Values are means ± SEM of three independent experiments. **p < 0.01 vs basal glucose uptake (no insulin stimulation); #p < 0.05 vs compound-treated basal glucose uptake; $p < 0.01 vs compound treated insulin-stimulated glucose uptake.

evidence that many natural products may be useful for treating DM in part, because they represent important sources of therapeutic compounds relevant for drug development (Huang et al., 2016; Yang et al., 2015; Zhao et al., 2017).

In the present study, we revealed that among the anthraquinone derivatives **(1–5)** isolated from *R. philippinensis*, MTAQ exhibited a significant and concentration-dependent reversible competitive inhibition of α-glucosidase activity. Additionally, MTAQ enhanced glucose uptake by activating insulin-mediated signaling and augmenting GLUT4 translocation in C2C12 myotubes. These findings suggest that MTAQ potentially represents a new hypoglycemic agent that can be used to treat T2-DM.

There is a pivotal role of α-glucosidase for metabolizing complex molecules of non-absorbable polysaccharide into intestinal absorbable monosaccharides. Thus, inhibition of α-glucosidase can result in the delayed conversion of complex polysaccharides to simple monosaccharides, leading to decreased glucose absorption and postprandial hyperglycemia, making it useful for studying the effects of nutraceuticals on T2-DM (Kim et al., 2005; Kwon et al., 2008; You et al., 2012). However, very few investigations have thoroughly explored the mode of action of α-glucosidase inhibitors. In this study, Lineweaver–Burk plots revealed that MTAQ inhibits α-glucosidase in a competitive manner, with $K^m$, $V^{max}$, and $K^i$ (at 50 μM) values of $6.42 \times 10^{-3}$ mM, $20.60 \times 10^{-2}$ ($\Delta A_{405}$ per min), and 41.88 μM, respectively.

The GLUT4 protein is one of the 14 members of the GLUT/SLC2A family of facilitative transmembrane hexose transporters, and is widely distributed in skeletal muscle, myocardium, fat, kidney, and brain. Additionally, insulin and muscle contractions induce the translocation of GLUT4 from GLUT4 vesicles in the cytoplasm to the plasma membrane, where it plays a pivotal role in the transport of glucose into the cell. Inhibited GLUT4 translocation to the plasma membrane is one of the important causes of insulin resistance in T2-DM (Govers, 2014; Lacombe, 2014). In the current study, we observed that MTAQ significantly increased glucose uptake *via* upregulated GLUT4 expression and increased translocation of the encoded protein in C2C12 cells (Figs. 3 and 4). Thus, MTAQ may be effective at alleviating insulin resistance in T2-DM.

We also sought to characterize the molecular mechanism underlying the induced production and translocation of GLUT4, which are mediated by insulin or exercise, ultimately leading to increased glucose uptake. In the insulin signaling pathway, IR is activated after interacting with insulin or IRS tyrosine residues, while PDK1 is phosphorylated, leading to the activation of PI3K and its downstream molecules, such as AKT, which stimulate GLUT4 translocation (Leto and Saltiel, 2012). Additionally, muscle contractions and/or AMPK activators, such as AICAR and metformin, activate the AMPK pathway in skeletal muscle by increasing the AMP:ATP ratio (O'Neill, 2013). In this study, MTAQ enhanced the phosphorylation of IRβ (Try 1150/1151), IRS-1 (S1101), PDK1, and AKT, whereas AMPK was unaffected (figure S3). Furthermore, to confirm whether MTAQ increases glucose uptake by activating AKT signaling, we analyzed the effects of LY294002, which is a specific AKT inhibitor. The phosphorylation of AKT and translocation of GLUT4 were significantly inhibited by LY294002 (Fig. 6). Moreover, LY294002 strongly attenuated basal and insulin-stimulated glucose uptake, indicating that IRS-1 downstream molecules and AKT are involved in MTAQ-induced insulin signaling. These results suggest that MTAQ may be useful for treating T2-DM because it can

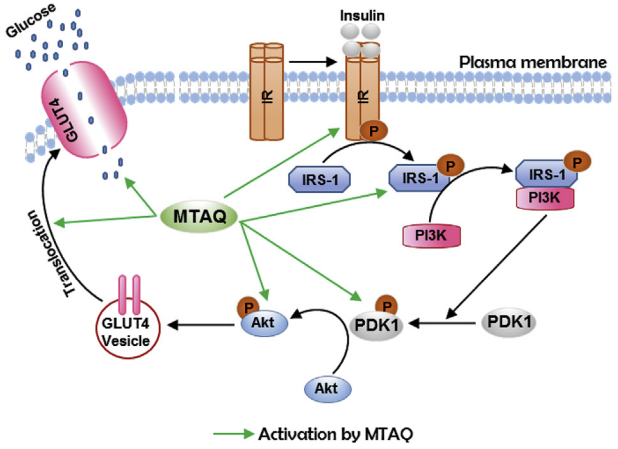


**Fig. 7.** Probable mechanism of action of MTAQ on glucose uptake through mimicking the insulin-signaling pathway.

mimic an insulin signal to activate the insulin-dependent pathway rather than the AMPK pathway (Fig. 7). Unlike the compounds investigated in a previous study (Nguyen et al., 2017), MTAQ is not an AMPK activator, possibly because of structural differences in specific moieties. Thus, additional studies are needed to confirm the role of AMPK functional groups and the underlying molecular mechanism.

## 5. Conclusions

In this study, we revealed that MTAQ strongly inhibited α-glucosidase in a competitive manner. It also enhanced GLUT4 translocation thus increased basal and insulin-stimulated uptake of glucose in C2C12 myotubes *via* an insulin-like signaling pathway rather than the AMPK pathway. To the best of our knowledge, this is the first report describing an anthraquinone isolated from *R. philippinensis* that is able to increase basal and insulin-stimulated uptake of glucose, therefore, convincing that MTAQ may be useful for developing novel insulin mimics capable of managing blood glucose levels.

## Declaration of conflict of interests

The authors have declared that there are no conflicts of interest.

## Acknowledgements

This study received financial support from the Basic Science Research Program through the National Research Foundation of Korea (NRF) funded by the Ministry of Science, ICT & Future Planning (2014R1A5A1009799). This study was also supported by the grant of Chungnam National University.

## Appendix A. Supplementary data

Supplementary data to this article can be found online at https://doi.org/10.1016/j.fct.2019.05.005.

## Transparency document

Transparency document related to this article can be found online at https://doi.org/10.1016/j.fct.2019.05.005.

## References

Ali, L., Khan, A.L., Al-Kharusi, L., Hussain, J., Al-Harrasi, A., 2015. New alpha-glucosidase inhibitory triterpenic acid from marine macro green alga codium dwarkense boergs. Mar. Drugs 13 (7), 4344–4356.
Bajpai, V.K., Alam, M.B., Quan, K.T., Choi, H.J., An, H., Ju, M.K., Lee, S.H., Huh, Y.S., Han, Y.K., Na, M., 2018. Cytotoxic properties of the anthraquinone derivatives isolated from the roots of *Rubia philippinensis*. BMC Complement Altern. Med. 18 (1) e200.
Collins, F.M., 2002. Current treatment approaches to type 2 diabetes mellitus: successes and shortcomings. Am. J. Manag. Care 8 (16 Suppl. l), S460–S471.
Echouffo-Tcheugui, J.B., Garg, R., 2017. Management of hyperglycemia and diabetes in the emergency department. Curr. Diabetes Rep. 17 (8), 56.
Gao, Y., Su, Y., Huo, Y., Mi, J., Wang, X., Wang, Z., Liu, Y., Zhang, H., 2014. Identification of antihyperlipidemic constituents from the roots of *Rubia yunnanensis* Diels. J. Ethnopharmacol. 155 (2), 1315–1321.
Gong, Y., Qin, X.Y., Zhai, Y.Y., Hao, H., Lee, J., Park, Y.D., 2017. Inhibitory effect of hesperetin on alpha-glucosidase: molecular dynamics simulation integrating inhibition kinetics. Int. J. Biol. Macromol. 101, 32–39.
Govers, R., 2014. Cellular regulation of glucose uptake by glucose transporter GLUT4. Adv. Clin. Chem. 66, 173–240.
Hesselink, M.K., Schrauwen-Hinderling, V., Schrauwen, P., 2016. Skeletal muscle mitochondria as a target to prevent or treat type 2 diabetes mellitus. Nat. Rev. Endocrinol. 12 (11), 633–645.
Huang, M., Zhao, P., Xiong, M., Zhou, Q., Zheng, S., Ma, X., Xu, C., Yang, J., Yang, X., Zhang, T.C., 2016. Antidiabetic activity of perylenequinonoid-rich extract from Shiraia bambusicola in KK-Ay mice with spontaneous type 2 diabetes mellitus. J. Ethnopharmacol. 191, 71–81.
Huang, S., Czech, M.P., 2007. The GLUT4 glucose transporter. Cell Metabol. 5 (4), 237–252.
Itokawa, H., Mihara, K., Takeya, K., 1983. Studies on a novel anthraquinone and its glycosides isolated from *Rubia cordifolia* and *R. akane*. Chem. Pharm. Bull. 31, 2353–2358.
Kim, Y.M., Jeong, Y.K., Wang, M.H., Lee, W.Y., Rhee, H.I., 2005. Inhibitory effect of pine extract on alpha-glucosidase activity and postprandial hyperglycemia. Nutrition 21 (6), 756–761.
Kwon, Y.I., Apostolidis, E., Shetty, K., 2008. In vitro studies of eggplant (Solanum melongena) phenolics as inhibitors of key enzymes relevant for type 2 diabetes and hypertension. Bioresour. Technol. 99 (8), 2981–2988.
Lacombe, V.A., 2014. Expression and regulation of facilitative glucose transporters in equine insulin-sensitive tissue: from physiology to pathology. ISRN Vet. Sci., 409547 2014.
Leto, D., Saltiel, A.R., 2012. Regulation of glucose transport by insulin: traffic control of GLUT4. Nat. Rev. Mol. Cell Biol. 13 (6), 383–396.
Li, Z.P., Song, Y.H., Uddin, Z., Wang, Y., Park, K.H., 2018. Inhibition of protein tyrosine phosphatase 1B (PTP1B) and alpha-glucosidase by xanthones from Cratoxylum cochinchinense, and their kinetic characterization. Bioorg. Med. Chem. 26 (3), 737–746.
Maritim, A.C., Sanders, R.A., Watkins 3rd, J.B., 2003. Diabetes, oxidative stress, and antioxidants: a review. J. Biochem. Mol. Toxicol. 17 (1), 24–38.
Nguyen, P.H., Choi, H.S., Ha, T.K.Q., Seo, J.Y., Yang, J.L., Jung, D.W., Williams, D.R., Oh, W.K., 2017. Anthraquinones from Morinda longissima and their insulin mimetic activities via AMP-activated protein kinase (AMPK) activation. Bioorg. Med. Chem. Lett 27 (1), 40–44.
O'Neill, H.M., 2013. AMPK and exercise: glucose uptake and insulin sensitivity. Diabetes Metab. J 37 (1), 1–21.
Quan, K.T., Park, H.S., Oh, J., Park, H.B., Ferreira, D., Myung, C.S., Na, M., 2016. Arborinane triterpenoids from *Rubia philippinensis* inhibit proliferation and migration of vascular smooth muscle cells induced by the platelet-derived growth factor. J. Nat. Prod. 79, 559–569.
Ross, S.A., Gulve, E.A., Wang, M., 2004. Chemistry and biochemistry of type 2 diabetes. Chem. Rev. 104 (3), 1255–1282.
Rozen, S., Skaletsky, H., 2000. Primer3 on the WWW for general users and for biologist programmers. Methods Mol. Biol. 132, 365–386.
Tundis, R., Loizzo, M.R., Menichini, F., 2010. Natural products as alpha-amylase and alpha-glucosidase inhibitors and their hypoglycaemic potential in the treatment of diabetes: an update. Mini Rev. Med. Chem. 10 (4), 315–331.
Whiting, D.R., Guariguata, L., Weil, C., Shaw, J., 2011. IDF diabetes atlas: global estimates of the prevalence of diabetes for 2011 and 2030. Diabetes Res. Clin. Pract. 94 (3), 311–321.
Xu, K., Wang, P., Wang, L., Liu, C., Xu, S., Cheng, Y., Wang, Y., Li, Q., Lei, H., 2014. Quinone derivatives from the genus Rubia and their bioactivities. Chem. Biodivers. 11 (3), 341–363.
Xu, K., Wang, P., Yuan, B., Cheng, Y., Li, Q., Lei, H., 2013. Structural and bioactive studies of terpenes and cyclopeptides from the Genus *Rubia*. Chem. Cent. J. 7 e81.
Yang, X., Yang, J., Xu, C., Huang, M., Zhou, Q., Lv, J., Ma, X., Ke, C., Ye, Y., Shu, G., Zhao, P., 2015. Antidiabetic effects of flavonoids from Sophora flavescens EtOAc extract in type 2 diabetic KK-ay mice. J. Ethnopharmacol. 171, 161–170.
You, Q., Chen, F., Wang, X., Jiang, Y., Lin, S., 2012. Anti-diabetic activities of phenolic compounds in muscadine against alpha-glucosidase and pancreatic lipase. LWT - Food Sci. Technol. 46 (1), 164–168.
Zhao, P., Alam, M.B., Lee, S.H., Kim, Y.J., Lee, S., An, H., Choi, H.J., Son, H.U., Park, C.H., Kim, H.H., Lee, S.H., 2017. Spatholobus suberectus exhibits antidiabetic activity in vitro and in vivo through activation of AKT-AMPK pathway. Evid. Based Complement. Altern. Med., 6091923 *2017*.
Zhou, Q.G., Hou, F.F., Guo, Z.J., Liang, M., Wang, G.B., Zhang, X., 2008. 1,25-Dihydroxyvitamin D improved the free fatty-acid-induced insulin resistance in cultured C2C12 cells. Diabetes Metab. Res. Rev. 24 (6), 459–464.